# Journal of Applied Sciences

ISSN 1812-5654

science alert

ANSInet
an open access publisher
http://ansinet.com

Journal of Applied Sciences 12 (3): 263-270, 2012
ISSN 1812-5654 / DOI: 10.3923/jas.2012.263.270


# Preparation of Surfactant-free Linear and Star-shaped Poly(L-lactide)-*b*-methoxy Polyethylene Glycol Nanoparticles for Drug Delivery

Yodthong Baimark
Department of Chemistry and Center of Excellence for Innovation in Chemistry, Faculty of Science, Mahasarakham University, Mahasarakham 44150, Thailand

**Abstract:** The objective of this research was to investigate the effect of arm number of Poly(l-lactide)-*b*-methoxy poly(ethylene glycol) (PLL-*b*-MPEG) amphiphilic diblock copolymers on their characteristics of drug-loaded nanoparticles and *in vitro* drug release. Linear and star-shaped PLL-*b*-MPEG diblock copolymers were synthesized via the ring-opening polymerization of L-lactide followed by coupling reaction with a monofunctional carboxyl end-group MPEG. These diblock copolymers included linear copolymer having one arm and star-shaped copolymers having four and six arms. The crystallinity of MPEG block within diblock copolymers was suppressed. The melting point ($T_m$) and degree of crystallinity ($\chi_c$) of PLL block within diblock copolymers decreased as the arm number increased. Drug-loaded nanoparticles of these copolymers were prepared by the emulsification-diffusion method under surfactant-free condition. Indomethacin was used as a poorly water-soluble model drug. The nanoparticles with less than 200 nm in size were nearly spherical shape. Different arm numbers did not affect average size and drug loading efficiency. However, the $T_m$ and $\chi_c$ of diblock copolymers slightly decreased after drug loading. From *in vitro* drug release test, drug release content increased steadily as the arm number increased.

**Key words:** Diblock copolymers, star-shaped polylactide, emulsification-diffusion method, nanoparticles, drug delivery

## INTRODUCTION

In recent year, there has been an increasing interest in biodegradable star-shaped polyesters of poly(L-lactide) (Wang and Dong, 2006; Zhang and Zheng, 2007), poly(D,L-lactide) (Srisa-ard and Baimark, 2010) and poly(ϵ-caprolactone) (Xie and Gan, 2009) which are branched polymers distinguished by a structure containing three or more linear arms radiating from a center. The star-shaped polyesters are expected to display peculiar viscosity, thermal and mechanical properties and degradation profiles compared with linear polyesters (Odelius and Ann-Christine, 2008). The polyesters with different arm numbers have been synthesized using initiators containing different hydroxyl end-groups. The chemical structures in each arm were the same. Influences of arm number and arm length on crystallinity, melting temperature and thermal degradation of these star-shaped polyesters have been reported.

Methoxy poly(ethylene glycol) (MPEG) blocks have been attached to polyester blocks as biodegradable amphiphilic diblock copolymers for increasing its hydrophilicity and flexibility. These amphiphilic diblock copolymers have been prepared as nanoparticle, film and tube forms for biomedical applications (Baimark *et al*., 2008; Srisuwan *et al*., 2008; Baimark and Phromsopha, 2009; Khamhan and Yodthong, 2009; Kotseang *et al*., 2009; Phromsopha and Baimark, 2009). Biodegradable amphiphilic MPEG-*b*-polyester diblock copolymers have been prepared as the surfactant-free nanoparticles for drug controlled release (Aliabadi *et al*., 2005; Baimark, 2009). These nanoparticles are core-shell structure with hydrophobic polyester core and hydrophilic MPEG shell. The MPEG blocks enhanced retention time of diblock copolymeric nanoparticles in the human blood system.

The star-shaped MPEG-*b*-polyester block copolymers have been synthesized and reported by many researchers (Cai *et al*., 2006; Lemmouchi *et al*., 2007; Wang *et al*., 2008; Lin and Zhang, 2010). However, the drug-loaded nanoparticle characteristics and drug release behaviors of the star-shaped MPEG-*b*-polyester block copolymers have been scarcely published (Quaglia *et al*., 2006).

In this study, the influence of arm number of poly(L-lactide)-b-MPEG (PLL-*b*-MPEG) on characteristics and drug release behaviors of drug-loaded PLL-*b*-MPEG nanoparticles was investigated. The PLL with arm numbers of 1, 4 and 6 were synthesized before coupling with carboxylic acid end-group MPEG.

## MATERIALS AND METHODS

This study was conducted on November 2010-October 2011 at Mahasarakham University, Mahasarakham, Thailand.

**Materials:** L-Lactide (LL) monomer was synthesized by well established procedure from L-lactic acid (88% Purac, Thailand). LL was purified by repeated recrystallization from distilled ethyl acetate for 4 times and dried in a vacuum oven at 45°C for 48 h before use. 1-dodeccanol (98%, Fluka, Switzerland) was purified by distillation under reduced pressure before being stored over molecular sieves. Pentaerythritol (99%, Aldrich, USA) and dipentaerythritol (99%, Aldrich, USA) were dried in a vacuum oven at 100°C for 24 h before use. Methoxy poly(ethylene glycol) (MPEG, Fluka, USA) with molecular weight of 5,000 g $mol^{-1}$ was dried at 120°C in a vacuum oven for 4 h before use. Stannous octoate ($Sn(Oct)_2$, 95% Sigma, USA), Dicyclohexylcarbodiimide (DCC, 99% Fluka, USA), 4-dimethylaminopyridine (DMAP, 99% Fluka, USA), succinic anhydride (99% Acros Organic, USA), triethylamine (99% Acros Organic) and indomethacin (99%, Sigma, USA) were used without further purification. All solvents in analytical grade were used.

**Synthesis of poly(L-lactide):** The poly(L-lactide)s (PLL) with arm numbers of 1, 4 and 6 were polymerized in bulk at 140°C for 24 h under nitrogen atmosphere. The 1-dodecanol, pentaerythritol and dipentaerythritol were used as hydroxyl end-group initiators to prepare linear, 4-armed and 6-arm PLLs, respectively. LL/initiator ratio of 208/1 by mole was used. The theoretical molecular weight of PLLs calculated from feed ratio was approximately 30,000 g $mol^{-1}$. Hydroxyl end-group compound and $Sn(Oct)_2$ were used as the initiating system. $Sn(Oct)_2$ concentration was kept constant at 0.02 mol%. The as-polymerized PLL was purified by being dissolved in chloroform before precipitating in cool n-hexane. The PLL was dried to constant weight in a vacuum oven at room temperature.

**Synthesis of carboxylic acid end-group methoxy poly(ethylene glycol):** Carboxylic acid end-group methoxy poly(ethylene glycol) (MPEG-COOH) was synthesized by changing a hydroxyl end-group of MPEG to a carboxylic acid end-group. For this purpose, MPEG (10 g, 2.0 mmol), succinic anhydride (304.8 mg, 3.0 mmol), DMAP (246.4 mg, 2.0 mmol) and triethylamine (203.6 mg, 2.0 mmol) were dissolved in dioxane (13 mL) and vigorous stirring for 48 h at room temperature. The solvent was then completely evaporated. The obtained residue was dissolved in methylene chloride before precipitating in ether. The precipitated MPEG-COOH was then dried in a vacuum oven at 40°C overnight.

**Synthesis of PLL-*b*-MPEG:** The linear and star-shaped PLL-*b*-MPEG diblock copolymers were prepared using the coupling reaction between the hydroxyl end-group of PLL and the carboxylic acid end-group of MPEG-COOH. The coupling reaction was illustrated in Fig. 1. For this purpose, PLL, MPEG-COOH, DCC and DMAP were dissolved in anhydrous methylene chloride (4.0 mL) and stirring for 48 h under nitrogen atmosphere at room temperature. The amounts of substances were summarized in Table 1. The acetone was added to precipitate dicyclohexylcarbodiurea by-product and residue DCC before filtering off. The filtered solution was dried by solvent evaporation. The dried solid was dissolved in chloroform before extraction with a 0.5 wt% HCl solution, followed by water. The obtained PLL-*b*-MPEG was dried over anhydrous $Na_2SO_4$ before evaporation.

**Characterization of PLL and PLL-*b*-MPEG:** The intrinsic viscosity, [η], of PLL and PLL-*b*-MPEG were determined from flow-time measurements on a diluted series of solutions in chloroform as solvent at 30°C using viscometrically. Molecular weight characteristics of the samples were characterized by Gel Permeation Chromatography (GPC) using a Waters 717 plus Autosampler GPC equipped with an Ultrastyragel® column operating at 40°C and employing universal calibration. Chloroform was used as the solvent at a flow rate of 1 mL $min^{-1}$. Thermal transition properties of the samples were carried out by means of Differential Scanning Calorimetry (DSC) using a Perkin-Elmer DSC Pyris Diamond. For DSC, the sample (3-5 mg) was sealed in aluminum pan before heated at 10°C/min under a helium atmosphere.

**Preparation of drug-loaded nanoparticles:** Surfactant-free drug-loaded PLL-*b*-MPEG nanoparticles were prepared via a nanoprecipitation method. Briefly, 5 mg of indomethacin and 80 mg of copolymer were dissolved in 8 mL of acetone/chloroform (7/1 v/v) mixture. The organic solution was added drop-wise into 80 mL of distilled water under

Table 1: Synthesis of PLL-*b*-MPEG by coupling reaction

| | | | MPEG-COOH (10% excess) | | DCC | | DMAP | |
|---|---|---|---|---|---|---|---|---|
| PLL | $M_{n,th}$[a] (g $mol^{-1}$) | 0.021 mmol PLL (mg) | mmol | mg | mmol | mg | mmol | mg |
| 1-arm | 30,000 | 630 | 0.0231 | 48.5 | 0.0277 | 5.6 | 0.0055 | 0.7 |
| 4-arm | 30,000 | 630 | 0.0924 | 194 | 0.1109 | 22.6 | 0.0222 | 2.8 |
| 6-arm | 30,000 | 630 | 0.1386 | 291.1 | 0.1663 | 33.9 | 0.0333 | 4.2 |

[a]The theoretical number-average molecular weight, as calculated from feed LL/initiator mole ratio

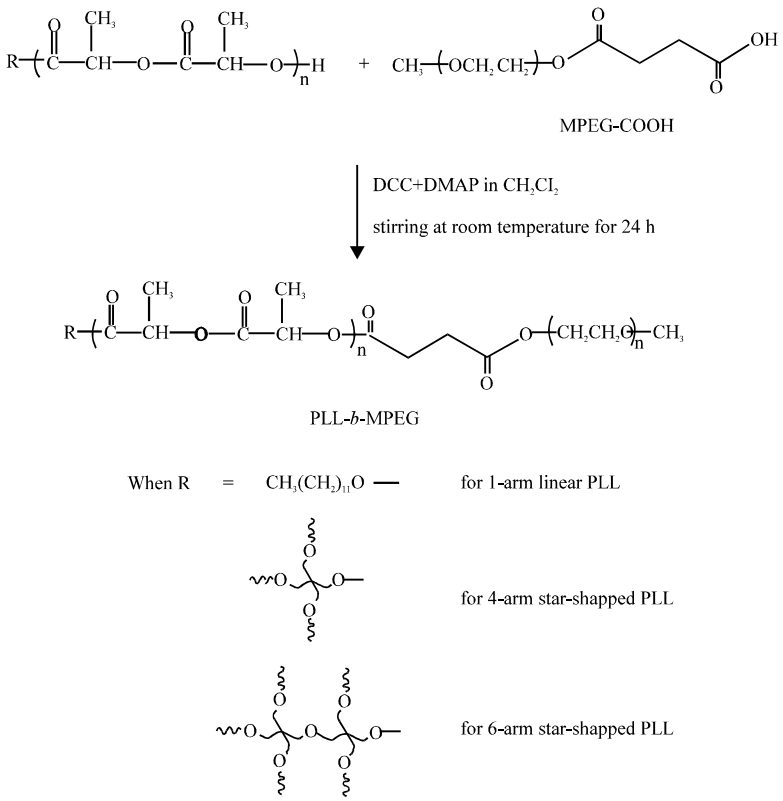


Fig. 1: Coupling reaction of PLL with MPEG-COOH

magnetic stirring. The nanoparticles were immediately formed after solvent diffusion. The organic solvents were then evaporated at room temperature for 6 h in a fume hood. The resultant nanoparticle suspension was centrifuged at 15,000 rpm 4°C for 2 h. The supernatant was carefully discarded and the precipitated nanoparticles were re-suspended in a phosphate buffer solution media (0.1 M, pH 7.4). The dried drug-loaded nanoparticles were obtained by freeze-drying the precipitated nanoparticles overnight.

**Characterization of drug-loaded nanoparticles:** Morphology of the drug-loaded nanoparticles was determined by Transmission Electron Microscopy (TEM) using a JEOL JEM 1230 TEM. For TEM analysis, a drop of nanoparticle suspension was placed on a formvar film coated on the copper grid. The specimen on the copper grid was not stained. Average particle size of the drug-loaded nanoparticles was measured from the nanoparticle suspension by Light Scattering (LS) analysis using a Coulter LS230 particle size analyzer at 25°C. Thermal transition properties of the freeze-dried nanoparticles were carried out by mean of DSC as described above.

Theoretical drug loading content ($DLC_{theoretical}$), actual drug loading content ($DLC_{actual}$) and Drug Loading Efficiency (DLE) were calculated from Eq. 1-3, respectively. The $DLC_{actual}$ is an average value from three measurements. For $DLC_{actual}$ measurement, the freeze-dried sample of drug-loaded nanoparticles was dissolved in dichloromethane. The weight of actual drug entrapped in the drug-loaded nanoparticles was determined by UV-vis spectrophotometry using a Perkin-Elmer Lambda 25 UV-vis spectrophotometer at 319 nm compared to standard curve of indomethacin:

$$DLC_{theoretical}(\%) = \frac{\text{Weight of feed drug}}{\text{Weights of feed drug and copolymer}} \times 100 \quad (1)$$

$$DLC_{actual}(\%) = \frac{\text{Weight of actual drug entrapped in nanoparticals}}{\text{Weights of drug-loaded nanoparticals}} \times 100 \quad (2)$$

$$DLE(\%) = \frac{DLC_{actual}}{DLC_{theoretical}} \times 100 \quad (3)$$

***In vitro* drug release test:** *In vitro* drug release from nanoparticles was performed by dialysis bag diffusion technique. Ten mL of drug-loaded nanoparticle re-suspension was placed in a dialysis bag, tied and

immersed into 100 mL phosphate buffer solution (0.1 M, pH 7.4). The entire system was kept at 37°C with horizontal shaking at about 150 rpm.

At predetermined time intervals, 5 mL of aliquots of the release medium were withdrawn from the release medium and the same volume of fresh buffer solution was added for continuing the drug release test. The concentration of indomethacin released was monitored using an UV-vis spectrophotometer at 319 nm. According to a predetermined indomethacin concentration-UV absorbance standard curve, indomethacin concentration of the release medium was obtained. Percentage of indomethacin release was calculated based on ratio of drug release in each release time and initial drug content within nanoparticles. The average % release was calculated from the three measurements.

## RESULTS

**Synthesis and characterization of PLL and PLL-*b*-MPEG:** The PLLs with different arms were synthesized through ring-opening polymerization of LL monomer by using different hydroxyl end-group compounds. The % yields of resultant linear (1-arm) and star-shaped (4-and 6-arm) PLLs after purification were higher than 95%. The intrinsic viscosity ([η]), number-average molecular weight ($M_n$) and Molecular Weight Distribution (MWD) of the PLLs are summarized in Table 2. It was found that the [η] of PLLs slightly decreased as the arm number increased, whereas the $M_n$ and MWD of the PLLs are in range of 25, 100-26, 500 g mol$^{-1}$ and 1.2-1.4, respectively. The PLL-*b*-MPEG was prepared by coupling hydroxyl end group of PLL with MPEG-COOH. The % yields of PLL-*b*-MPEG were higher than 90%. The [η], $M_n$ and MWD of PLL-*b*-MPEG are also reported in Table 2. The [η] and $M_n$ of PLL increased but MWD did not after coupling with MPEG-COOH. It should be noted that the increasing of [η] and $M_n$ of PLL after coupling MPEG-COOH are in order 6-arm>4-arm >1-arm PLL.

Thermal transition properties such as a melting temperature ($T_m$) and a heat of melting ($\Delta H_m$) of the PLL and PLL-*b*-MPEG were determined from DSC analysis. The DSC results are reported in Table 3. The $T_m$ and $\Delta H_m$ of PLLs decreased significantly when the arm number was increased. Degree of crystallinity ($\chi_c$) of the PLLs directly related to its $\Delta H_m$ is also summarized in Table 3 that decreased as the arm number increased. DSC thermograms of the PLL-*b*-MPEG are shown in Fig. 2. The $T_m$, $\Delta H_m$ and $\chi_c$ of the PLL-*b*-MPEG were slightly lower than the starting PLL. The higher arm number PLL-*b*-MPEG showed lower $T_m$ and $\Delta H_m$. In addition, the crystallinity of MPEG block was suppressed after coupling with PLL.

Table 2: Intrinsic viscosity and molecular weight characteristics of PLL and PLL-*b*-MPEG

| Sample | [η] (dL g$^{-1}$)[a] | Mn (g mol$^{-1}$)[b] | MWD[b] |
|---|---|---|---|
| 1-arm PLL | 0.4483 | 25,100 | 1.4 |
| 4-arm PLL | 0.3172 | 25,400 | 1.2 |
| 6-arm PLL | 0.3095 | 26,500 | 1.2 |
| 1-arm PLL-b-MPEG | 0.4624 | 27,400 | 1.4 |
| 4-arm PLL-b-MPEG | 0.4012 | 48,700 | 1.3 |
| 6-arm PLL-b-MPEG | 0.4261 | 57,800 | 1.1 |

[a]Intrinsic viscosity ([η]) was determined at 30°C using chloroform as the solvent. [b]Number-average molecular weight ($M_n$) and Molecular Weight Distribution (MWD) were measured from GPC analysis

Table 3: Thermal transition properties of PLL and PLL-*b*-MPEG

| Sample | $T_m$ (°C)[a] | $\Delta H_m$ (J/g)[a] | $\chi_c$ (%)[b] |
|---|---|---|---|
| 1-arm PLL | 170 | 60.7 | 64.9 |
| 4-arm PLL | 161 | 42.5 | 45.4 |
| 6-arm PLL | 156 | 35.6 | 38 |
| 1-arm PLL-b-MPEG | 169 | 56.4 | 60.2 |
| 4-arm PLL-b-MPEG | 160 | 37.8 | 40.4 |
| 6-arm PLL-b-MPEG | 154 | 31.2 | 33.3 |

[a]Melting temperature ($T_m$) and heat of melting ($\Delta H_m$) were determined from DSC analysis. [b]Degree of crystallinity ($\chi_c$) was calculated from $\chi_c = [\Delta H_m/93.6]\times100$

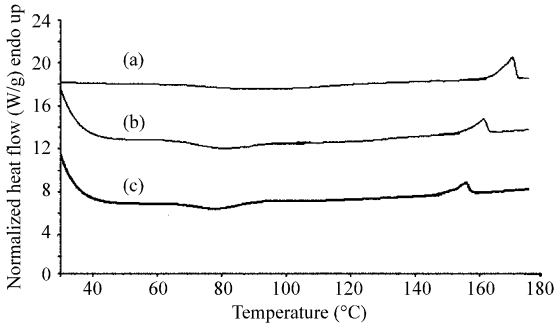


Fig. 2: DSC thermograms of (a) 1-arm PLL-*b*-MPEG, (b) 4-arm PLL-*b*-MPEG and 6-arm PLL-*b*-MPEG

**Preparation and characterization of drug-loaded nanoparticles:** The surfactant-free PLL-*b*-MPEG nanoparticles containing indomethacin were prepared by the nanoprecipitation. The morphology of drug-loaded nanoparticles was determined from TEM micrographs as shown in Fig. 3. It can be seen that they were nearly spherical in shape. The average size of nanoparticles was measured by light-scattering analysis, as example of which is shown in Fig. 4 for the drug-loaded nanoparticles of linear PLL-*b*-MPEG. The particle sizes were less than 200 nm with narrow size distribution. The average sizes of drug-loaded nanoparticles of PLL-*b*-MPEG are reported in Table 4. They were in range of 118-128 nm. This indicates that the arm number of PLL-*b*-MPEG did not affect average particle size of the drug-loaded nanoparticles. The $T_m$ and $\Delta H_m$ of nanoparticles determined from DSC thermograms in Fig. 5 and reported in Table 4 were slightly lower than its PLL-*b*-MPEG (Table 3).

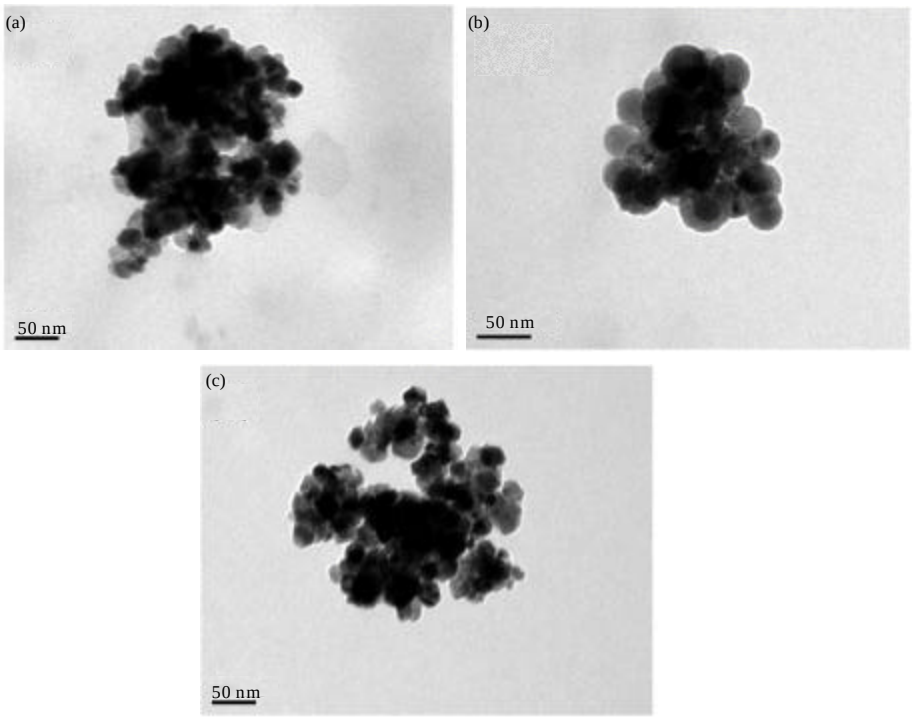


Fig. 3(a-c): TEM images of drug-loaded nanoparticles of (a) 1-arm PLL-*b*-MPEG, (b) 4-arm PLL-*b*-MPEG and (c) 6-arm PLL-*b*-MPEG. All bars = 50 nm

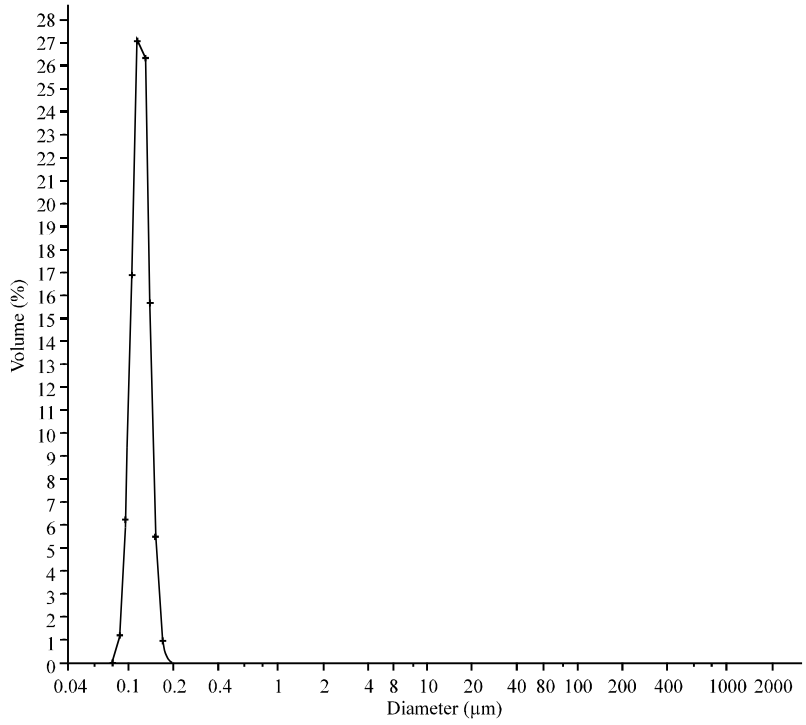


Fig. 4: Particle size graph of drug-loaded 1-arm PLL-*b*-MPEG nanoparticles

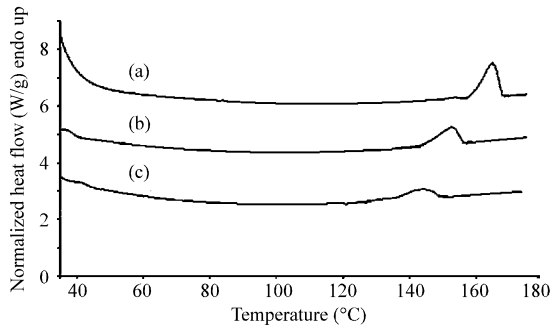


Fig. 5: DSC thermograms of drug-loaded nanoparticles of (a) 1-arm PLL-*b*-MPEG, (b) 4-arm PLL-*b*-MPEG and (c) 6-arm PLL-*b*-MPEG

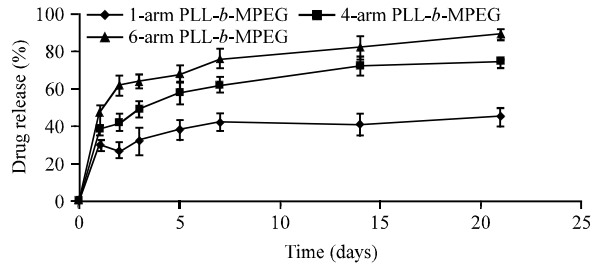


Fig. 6: Drug release profiles from nanoparticles of 1-arm PLL-*b*-MPEG, 4-arm PLL-*b*-MPEG and 6-arm PLL-*b*-MPEG

Table 4: Average particle size and drug content of drug-loaded nanoparticles

| Drug-loaded nanoparticles | Average size[b] ±SD (nm) | $T_m$[a] (°C) | $\Delta h_m$[a] (J/g) | $DLC_{actual}$[c] (%) | DLE[c] (%) |
|---|---|---|---|---|---|
| 1-arm PLL-b-MPEG | 128±14 | 165 | 37.9 | 2.45 | 42 |
| 4-arm PLL-b-MPEG | 127±23 | 153 | 26.4 | 2.11 | 36 |
| 6-arm PLL-b-MPEG | 118±18 | 143 | 21.2 | 2.48 | 42 |

[a]Melting temperature ($T_m$) and heat of melting ($\Delta H_m$) were determined from DSC analysis. [b]Average particle size was measured from light-scattering analysis. [c]Actual drug loading content ($DLC_{actual}$) and Drug Loading Efficiency (DLE) were calculated from Eq. 2 and 3, respectively

The theoretical drug loading content ($DLC_{theoretical}$) of the drug-loaded nanoparticles calculated from Eq. 1 is 5.88%. The actual drug loading content ($DLC_{actual}$) and Drug Loading Efficiency (DLE) of the drug-loaded nanoparticles were calculated from Eq. 2 and 3, respectively that are also summarized in Table 4. The $DLC_{actual}$ and DLE of the drug-loaded nanoparticles are similar that in range of 2.11-2.48 and 36-42%, respectively.

***In vitro* drug release:** Figure 6 shows *in vitro* drug release patterns from PLL-*b*-MPEG nanoparticles with different arm numbers in phosphate buffer solution pH 7.4 at 37°C for 21 days. It can be clearly observed that the drug release profiles exhibit biphasic containing rapid initial burst release within the first day of release time followed with sustained release. The % drug releases at 21 days of release time are 41, 72 and 82% for 1-, 4-and 6-arm PLL-*b*-MPEG nannoparticles, respectively. The drug release significantly increased as the arm number increased. The results suggested that the drug release pattern strongly depended upon the arm number of PLL-*b*-MPEG.

## DISCUSSION

**Synthesis and characterization of PLL and PLL-*b*-MPEG:** The hydroxyl end-group compound/$Sn(Oct)_2$ system has been widely used to polymerize the LL monomer (Aliabadi *et al*., 2005; Wang and Dong, 2006). The shape or arm number of PLL depended upon the hydroxyl group of co-initiator. The 1-dodecanol, pentaerythritol and dipentaerythritol containing 1, 4 and 6 hydroxyl end-groups have used to prepare 1-, 4-and 6-arm PLLs, respectively (Srisa-ard and Baimark, 2010). The high % yields (>95%) of PLLs in this work suggested that the polymerization condition (140°C for 24 h) was appropriate. Table 2 reports the [η], $M_n$ and MWD of the PLLs and PLL-*b*-MPEG. The [η] of PLL decreased steadily as the arm number increased. The [η] of PLL solution directly related to hydrodynamic volume of PLL molecule in solution state. The higher arm number polyester exhibited smaller hydrodynamic volume (Wang and Dong, 2006; Srisa-ard and Baimark, 2010). The hydrodynamic volume of PLL molecules decreased as the arm number increased for the similar molecular weight. Thus, the higher arm number PLL induced lower the [η] value. However, the $M_n$ and MWD of these PLLs from GPC are similar.

For PLL-*b*-MPEG preparation, the hydroxyl end-group of PLL was reacted with carboxylic acid end-group of MPEG-COOH, as shown in Fig. 1. The [η] and $M_n$ of PLL-*b*-MPEG in Table 2 were higher than the starting PLL for the same arm number. The results supported that the PLL reacted with MPEG to form as the block copolymer. The coupling reaction did not affect the MWD. The 6-arm PLL-*b*-MPEG showed the highest increasing of [η] and $M_n$. This may be due to the 6-arm PLL contained 6 hydroxyl end-groups that connected to 6 molecules of MPEG-COOH according to the literature (Wang *et al*., 2008).

From DSC results in Table 3, it can be seen that the 1-arm PLL exhibited the highest $T_m$, $\Delta H_m$ and $\chi_C$ values. These values of the PLL decreased as the arm number increased according to the literatures (Wang and Dong, 2006; Zhang and Zheng, 2007). The arm length of 1-arm PLL was longer than the 4-and 6-arm PLLs. The longer arm length PLL induced higher $T_m$, $\Delta h_m$ and $\chi_C$. For PLL-*b*-

PEG, these thermal properties slightly decreased when the PLL block was attached to MPEG block. The MPEG block may inhibit crystallizing of PLL block. Moreover, the crystallinity of MPEG block within PLL-*b*-MPEG disappeared. This confirmed the attachment between PLL and MPEG blocks. The rigid PLL blocks prevented crystallization of flexible MPEG blocks. Suppression of MPEG crystallizability by copolymerizing poly(D,L-lactide) block has been reported in our previous works (Kotseang *et al*., 2009; Baimark and Phromsopha, 2009).

**Preparation and characterization of drug-loaded nanoparticles:** The emulsification-diffusion method was used to prepare the surfactant-free nanoparticles of amphiphilic diblock copolymers using acetone/chloroform mixture as the organic solvent. The MPEG blocks can act as stabilizer to prevent nanoparticle aggregation (Baimark *et al*., 2008). The core-shell nanoparticles with nearly spherical shape were formed. From Table 4, the drug-loaded nanoparticles with 118-128 nm in size were prepared with narrow size distribution. The results suggested that the MPEG blocks of PLL-*b*-MPEG with different arm numbers showed similar effective to stabilize the nanoparticle formation.

The $T_m$ and $\Delta H_m$ of the PLL-*b*-MPEG (Table 3) were slightly decreased in the nanoparticle matrix form (Table 4). This may be due to the drug molecules distributed into the nanoparticles that inhibited crystallizing of PLL-*b*-MPEG. However, the arm number of PLL-*b*-MPEG did not affect the DLE of nanoparticles.

***In vitro* drug release:** The effect of arm numbers of PLL-*b*-MPEG on *in vitro* drug release behavior from PLL-*b*-MPEG nanoparticles are illustrated in Fig. 6. The rapid initial burst release within the first day from the nanoparticles was probably due to the releasing of drug that entrapped on the nanoparticle surfaces. After that the sustain release may be due to drug diffusion mechanism through nanoparticle matrix. The drug release contents are in order 6-arm>4-arm>1-arm PLL-*b*-MPEG. This may be explained that the drug can easier diffuse through the amorphous phase than the crystalline phase. From Table 3, the crystallinity values of PLL-*b*-MPEG are in order 1-arm>4-arm>6-arm PLL-*b*-MPEG. Thus the amorphous values of PLL-*b*-MPEG are in order 6-arm>4-arm>1-arm PLL-*b*-MPEG.

## CONCLUSION

In the present study, the nanoparticles of linear and star-shaped PLL-*b*-MPEG were prepared by the emulsification-diffusion method for controlled-release of a poorly water-soluble model drug, indomethacin. The drug-loaded nanoparticles with less than 200 nm in size had nearly spherical in shape. The different arm numbers of PLL-*b*-MPEG did not affect the average size, shape and DLE of the drug-loaded nanoparticles. However, the drug release contents from PLL-*b*-MPEG nanoparticles were in order 6-arm>4-arm>1-arm PLL-*b*-MPEG. Therefore, the drug release rate can be tailored by varying the arm number of PLL-*b*-MPEG nanoparticle matrix. These nanoparticles may have potential to provide other poorly water-soluble drugs for use as controlled-release drug delivery systems.

## ACKNOWLEDGEMENTS

This study was supported by the Mahasarakham University and the Center of Excellence for Innovation in Chemistry (PERCH-CIC), Commission on Higher Education, Ministry of Education, Thailand.

## REFERENCES

Aliabadi, H.M., A. Mahmud, A.D. Sharifabadi and A. Lavasanifar, 2005. Micelles of methoxy poly(ethylene oxide)-*b*-poly(ε-caprolactone) as vehicles for the solubilization and controlled delivery of cyclosporine A. J. Control. Release, 104: 301-311.

Baimark, Y. and T. Phromsopha, 2009. Methoxy poly ethylene glycol-*b*-poly (D, L-lactide-co-glycolide) films as drug delivery systems for ibuprofen. Asian J. Sci. Res., 2: 87-95.

Baimark, Y., 2009. Surfactant-free nanospheres of methoxy poly (ethylene glycol)-*b*-poly (ε-caprolactone) for controlled release of ibuprofen. J. Applied Sci., 9: 2287-2293.

Baimark, Y., Y. Srisuwan, N. Kotsaeng and P. Threeprom, 2008. Preparation of surfactant-free and core-shell type nanoparticles of methoxy poly(ethylene glycol)-*b*-poly ε-caprolactone-co-D, L-lactide diblock copolymers. Asian J. Applied Sci., 1: 237-245.

Cai, C., L. Wang and C.M. Dong, 2006. Synthesis, characterization, effect of architecture on crystallization and spherulitic growth of poly(L-lactide)-*b*-poly(ethylene oxide) copolymers with different branch arms. J. Polym. Sci., Part A: Polym. Chem., 44: 2034-2044.

Khamhan, S. and B. Yodthong, 2009. Morphology and thermal stability of chitosan and methoxy poly (ethylene glycol)-*b*-poly (ε-caprolactone)/poly (D, L-lactide) nanocomposite films. J. Applied Sci., 9: 1147-1152.

Kotseang, N., Y. Srisuwan and Y. Baimark, 2009. Preparation and *in vitro* degradation of methoxy poly(ethylene glycol)-*b*-poly(D, L-lactide) tubes for nerve tissue engineering. Int. J. Chem. Technol., 1: 26-32.

Lemmouchi, Y., M.C. Perry, A.J. Amass, K. Chakraborty and E. Schacht, 2007. Novel synthesis of biodegradable star poly(ethylene glycol)-block-poly(lactide) copolymers. J. Polym. Sci., Part A: Polym. Chem., 45: 3966-3974.

Lin, Y. and A. Zhang, 2010. Synthesis and characterization of star-shaped poly(d, l-lactide)-block-poly(ethylene glycol) copolymers. Polym. Bull., 65: 883-892.

Odelius, K. and A. Ann-Christine, 2008. Precision synthesis of microstructures in star-shaped copolymers of caprolactone, L-lactide, and 1,5-dioxepan-2-one. J. Polymre Sci. Part A, 46: 1249-1264.

Phromsopha, T. and Y. Baimark, 2009. Methoxy poly(ethylene glycol)-*b*-poly(D, L-lactide) films for controlled release of ibuprofen. Trends Applied Sci. Res., 4: 107-115.

Quaglia, F., L. Ostacolo, G. De Rosa, M.I. La Rotonda and M. Ammendola *et al*., 2006. Nanoscopic core-shell drug carriers made of amphiphilic triblock and star-diblock copolymers. Int. J. Pharm., 324: 56-66.

Srisa-ard, M. and Y. Baimark, 2010. Effects of arm number and arm length on thermal properties of linear and star-shaped poly(D, L-lactide)s. J. Applied Sci., 10: 1937-1943.

Srisuwan, Y., M. Srisa-ard, C. Sittiwet, Y. Baimark, N.A. Narkkong and C. Butiman, 2008. Preparation and characterization of nanocomposite and nanoporous silk fibroin films. J. Applied Sci., 8: 2258-2264.

Wang, H.B., X.S. Chen and C.Y. Pan, 2008. Synthesis and micellization of star-like hyperbranched polymer with poly(ethylene oxide) and poly(ε-caprolactone) arms. J. Polym.Sci. Part A: Polym. Chem., 46: 1388-1401.

Wang, L. and C.M. Dong, 2006. Synthesis, crystallization kinetics, and spherulitic growth of linear and star-shaped poly(L-lactide)s with different numbers of arms. J. Polymer Sci. Part A: Polymer Chem., 44: 2226-2236.

Xie, W. and Z. Gan, 2009. Thermal degradation of star-shaped poly(ε-caprolactone). Polymer Degrad. Stab., 94: 1040-1046.

Zhang, W. and S. Zheng, 2007. Synthesis and characterization of dendritic star poly(L-lactide)s. Polymer Bull., 58: 767-775.